SCIENCE CHINA
Life Sciences

CrossMark
click for updates

•RESEARCH PAPER•

January 2021 Vol.64 No.1: 144–151
https://doi.org/10.1007/s11427-020-1726-5

Cue-triggered activity replay in human early visual cortex

Junshi Lu[1,2], Lu Luo[1,2], Qian Wang[1,3], Fang Fang[1,2,4*] & Nihong Chen[5,6*]

[1]*School of Psychological and Cognitive Sciences and Beijing Key Laboratory of Behavior and Mental Health, Peking University, Beijing 100871, China;*
[2]*IDG/McGovern Instituten*

March 23, 2020; accepted May 9, 2020; published online une 16, 2020

The recall of learned temporal se uences by a visual cue is an important form of experience-based neural plasticity. Here we observed such reactivation in awake human visual cortex using intracranial recording. fter repeated exposure to a moving dot, a flash of the dot was able to trigger neural reactivation in the downstream receptive field along the motion path. This effect was observed only when the cue appeared near the receptive field. The estimated traveling speed was faster compared to the activation induced by the real motion. e suggest a range-limited, time-compressed reactivation as a result of repeated visual exposure in awake human visual cortex.

sEEG, replay, visual cortex, neural plasticity

Citation: Lu, J., Luo, L., Wang, Q., Fang, F., and Chen, N. (2021). Cue-triggered activity replay in human early visual cortex. Sci China Life Sci 64, 144–151. https://doi.org/10.1007/s11427-020-1726-5

INTRODUCTION

Reactivation of stimulus-induced neuronal activity is a phenomenon by which neurons in selected brain regions exhibit specific activation patterns that resemble responses evoked by previous stimulation (Foster, 2017). The re-emergence of activity patterns occurs not only during periods of sleep (Wilson and McNaughton, 1994; Ji and Wilson, 2007), but also in the restful awake state (Foster and Wilson, 2006; Karlsson and Frank, 2009). Such experience-based reactivation reflects a "memory trace" in the brain, which plays a critical role in learning and memory consolidation.

The recall of a temporal sequence is a fundamental form of experience-based reactivation that can be used to predict future events based on current sensory inputs in the dynamic world (Fortin et al., 2002; de Lange et al., 2018). Activity replay of serially ordered temporal sequences has been first observed in the hippocampus and its surrounding cortical areas (Wilson and McNaughton, 1994; Gelbard-Sagiv et al., 2008). More recent electrophysiological studies have suggested that sequential recall could be a universal mechanism in the brain that also occurs in the sensory cortex (Bahramisharif et al., 2018; Lisman and Jensen, 2013). In the visual domain, involuntary sequential recalls have been found in the striate and extrastriate cortex, after repeated exposure with a simple moving dot (Xu et al., 2012), orientation or image sequences (Han et al., 2008; Eagleman and Dragoi, 2012; Gavornik and Bear, 2014; Liu et al., 2019), and natural movies (Yao et al., 2007; Chelaru et al., 2016).

While sequential reactivation is crucial for learning and prediction, there is only limited information about the se-

*Corresponding authors (Fang Fang, email: ffang@pku.edu.cn; Nihong Chen, email: nihongch@mail.tsinghua.edu.cn)

quential replay in human. A growing body of research has reported involuntary reactivation of serially ordered visual sequence in the visual cortex, mostly in mammals and non-human primates (Gavornik and Bear, 2014; Han et al., 2008; Eagleman and Dragoi, 2012; Xu et al., 2012; but see Chelaru et al., 2016; Liu et al., 2019). In human, most research has focused on the replay during active working memory tasks (e.g., Deuker et al., 2013; Jafarpour et al., 2014; Huang et al., 2018). Meanwhile, the neural mechanisms of involuntary sequential replay remain unclear in human sensory cortex.

To provide electrophysiological evidence of sequential reactivation in the human brain, we conducted intracranial recordings using stereo-electroencephalogram (sEEG) in awake human V1–V3. We applied a conditioning paradigm in which subjects viewed a moving dot repeatedly (Xu et al., 2012). Before and after repeated exposure of a moving dot, we compared sEEG activity evoked by a flash of the dot at different positions along the motion trajectory.

RESULTS

Conditioning

The main experiment was set up according to the spatial receptive field (RF) properties of every electrode contact which produced a spatially restricted and short-latency response to high-contrast checkerboard stimuli (Yoshor et al., 2007). Receptive fields were reliably mapped in eight electrode contacts from three subjects (Table 1). Based on the anatomical retinotopic template (Benson et al., 2014), these electrode contacts were located in V1–V3 (Figure 1B). During the conditioning phase, a bright dot moved repeatedly from a starting point (S) to an end point (E), with RF in between (Figure 1A). We observed visual evoked potentials (VEPs) evoked by the stimulus in each contact (Figure 2A). Across eight individual contacts, the averaged latency of VEPs was significantly correlated with the physical moving time from the starting point to the RF boundary (r=0.74, P=0.036). This result confirmed that the estimation of the RF size and location from the independent receptive field mapping session was accurate.

We performed a spectrotemporal analysis on the responses in the conditioning phase (Figure 2B). Notably, during the visual stimulation period, the amplitude increased in a frequency range from 30 to 60 Hz. This increase was reliable across contacts and subjects, consistent with the important role of gamma-frequency oscillations in sensory processing (Tallon-Baudry and Bertrand, 1999; Bartoli et al., 2019; Zhang et al., 2020). Our further analyses focused on the gamma-band signals at Pre and Post to test whether the conditioning led to a cortical replay that resembles the responses evoked by the moving dot.

Cue-triggered activity recall

Before (Pre) and after (Post) the conditioning, a dot was presented at one of four possible locations: S (starting point), A and B (trisection points of line S-RF), and E (end point) (Figure 1A). To illustrate the traveling direction of the activity recall, we computed the correlation between the time-series responses of each test condition and S (i.e., S-S, S-A, S-B, S-E) across different time lags. Then, we plotted the cross-correlogram against the time lags and the positions (S/A/B/E) in a distance-ascending order (Figure 3). S was chosen as a reference because it was the starting point, and a slant in the cross-correlogram reflects the spreading direction of the response.

A lower left to upper right slant of the correlation functions represents a gradual shift in the relative response timing at RF as the test position shifted from S to B (i.e., when a cue flashed at B, the response timeseries need to be adjusted ahead to have the highest correlation with the response timeseries evoked by a cue flashed at S). At Pre, the peak of correlation coefficients showed a slight rightward shift. This is because the response to a flashed stimulus generally shows some horizontal spread in the cortex (Bringuier et al., 1999). Similar patterns have been found in the rat electrophysiological study before conditioning (Xu et al., 2012). At Post, we observed a marked increase in the slant (S→B) after conditioning, which serves as a reliable indicator for se-

Table 1 sEEG recording sites

Contact No.	Subject No.	*X*	*Y*	*Z*	Region	RF size (°)
1	1	−6	−74	0	V1	1.20
2	1	−10	−74	0	V2	1.74
3	2	−10	−74	−7	V2	1.60
4	2	−16	−72	−8	V2	1.99
5	2	−19	−73	−8	V2	1.88
6	2	−22	−74	−8	V2	1.58
7	2	−26	−75	−8	V3	2.48
8	3	−3	−78	−10	V2	2.55

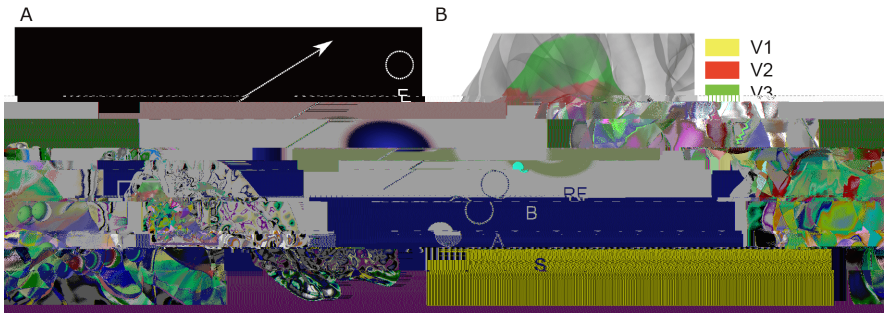

Figure 1 Schematic illustration of experimental stimuli and recording sites. A, Schematic illustration of stimuli. The conditioning stimulus consisted of a bright dot moved from S to E, with RF (red ellipse) in between. The test stimulus flashed at four positions (S, A, B, E) along the motion trajectory. The stimulus configuration varied according to the RF location of the recording contact, with the distance between S and E fixed at 24° and RF being the midpoint between S and E. The yellow dot at the center of the visual field serves as the fixation point. B, sEEG recording sites. Eight electrode contacts from three subjects were shown on a standard cortical surface. See Table 1 for coordinates and receptive field size of each electrode contact.

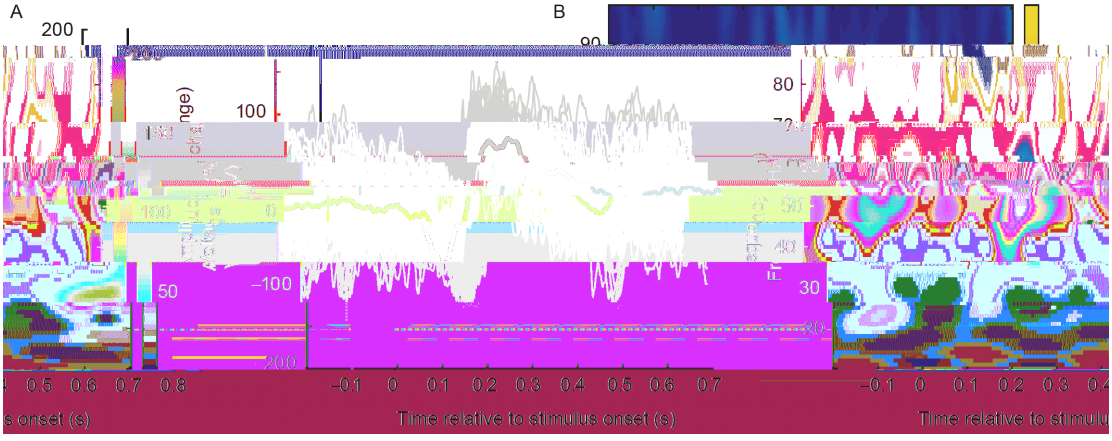

Figure 2 Response evoked by a moving dot in the conditioning phase. A, Averaged VEP (black curve) across individual trials (gray curve) in an example electrode contact. Black vertical line indicates stimulus onset. B, Time-frequency power profile (spectrogram) for the conditioning stimuli from the same example electrode contact. Color map reflects percentage change in amplitude relative to the pre-stimulus period.

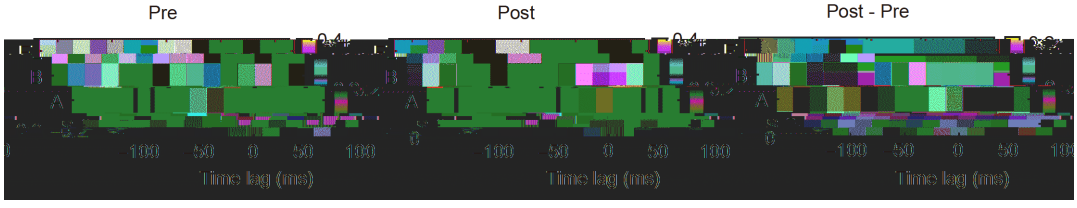

Figure 3 Cross-correlogram of gamma-band responses. The cross-correlograms at Pre (left panel) and Post (middle panel) showed averaged correlation coefficient across contacts, plotted against the time lags and cue positions. Right panel shows difference in the cross-correlograms before and after conditioning.

quential activation along the moving direction. In contrast, the correlation coefficient distribution at E has no marked peak. A permutation test for the difference plot showed that there was a significant increase at 46.9–62.5 ms post stimulus onset for condition A, and 62.5–93.8 ms for condition B. These results indicate that the motion conditioning enhanced test cue-evoked sequential responses of the cortical ensemble in the S→E direction.

To test whether a brief cue outside the RF would elicit a response in the RF after conditioning, we compared the gamma amplitudes in individual electrode contacts between Pre and Post (Figure 4). An electrode contact was considered to have a significant conditioning effect if the data from Pre and Post differed over a 30 ms time window (paired *t*-test, $P<0.05$) within 0–200 ms post stimulus onset. In S1 and S2, a significant conditioning effect was found in 4 out of 7 contacts when the cue flashed at position B. In S3, a significant conditioning effect was found when the cue flashed at position A in the only one contact. Of note, the RF of the contact in S3 was large and extended to position B, thus a cue

at position B evoked responses with similar amplitudes at Pre and Post.

Next, we performed a group-level analysis across the electrode contacts (Figure 5A). The cue positions were labeled into four categories: S (Start point), SF (Starting side, Far from the RF), SN (Starting side, Near the RF) and E (End point). S and E were the same as previously defined. In S1 and S2, SF and SN corresponded to position A and B, respectively. In S3, SF and SN corresponded to position S and A, respectively, because position B fell in the receptive field of the recording neural populations. We calculated the peak amplitude of the responses averaged across trials at each cue position. Repeated measures ANOVA showed a significant interaction effect between cue position and test phase (F(3,18)=3.68, P=0.032). Relative to Pre, a significant response increase was found only at SN (t(7)=2.57, P=0.037). No significant response increase was observed at S, SF, or E (all t(7)<1.85, P>0.10). The lack of response increase at position S and SF suggests that the replay could only be triggered within a limited range.

In addition, we computed the peak amplitudes of the broadband (8–240 Hz) signal and compared the responses between Pre and Post. Similarly, there was a significant interaction between test phase and cue position (F(3,21)

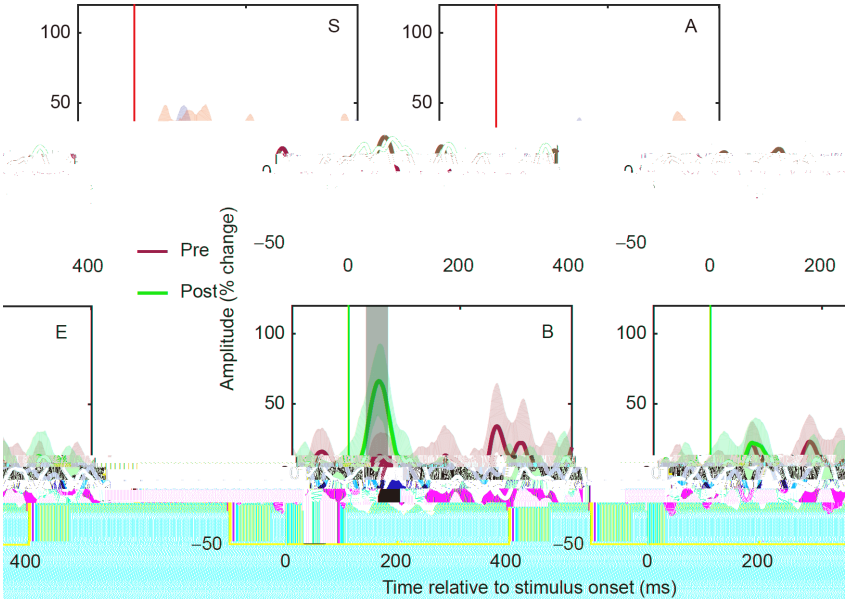

Figure 4 Gamma responses evoked by a cue flashed at different positions along the motion trajectory. Responses were measured as gamma amplitude (percent change from baseline) from an example electrode contact (C1). Red line indicates stimulus onset. Color shading indicates the 95% confidence interval. Gray shading indicates significant differences between Pre and Post (P<0.05, paired t-test). See Figure S1 in Supporting Information for all individual data.

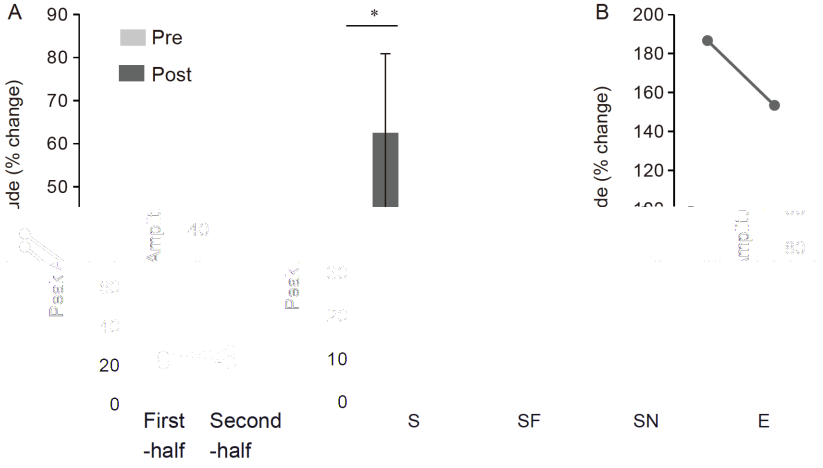

Figure 5 Cue-triggered responses before and after conditioning. A, Peak amplitude before and after conditioning, derived from gamma band signals in a 0–200 ms window post stimulus onset. Data were averaged across all 8 electrode contacts. Error bar indicates 1 SEM across contacts. B, Peak amplitude in the SN condition in the first and second halves of trials after conditioning.

=11.49, $P<0.001$). An elevated response after conditioning was found at SN ($t(7)=4.06$, $P=0.005$), but not at other cue positions (all $t(7)<1.84$, $P>0.10$). These results suggest that the activity recall could be induced across a wide frequency range after conditioning.

Temporal dynamics of activity recall

We further examined the temporal characteristics of the cue-triggered replay in two aspects. First, we tested whether the neural activity of the recalled motion sequence propagated at a different speed from that evoked by the physical motion. For each electrode contact, the recall latency was defined as the latency of gamma-band response triggered by a dot flash at SN in the post-test phase. The physical latency was defined as the latency of gamma-band response triggered by the moving dot in the conditioning phase (the onset time was adjusted to make SN as the starting point). A temporal compression ratio was calculated by dividing the physical latency by the recall latency (Figure 6). The resulting compression rate was 1.54±0.26 (mean±SEM), which was significantly greater than 1 ($t(4)=4.63$, $P=0.01$). This result suggests that the cue-triggered recall was accelerated in time.

To assess whether the cue-triggered response decayed over time, we split the post-conditioning trials in each block into two halves over time (Figure 5B). Each half lasted for 90 s. The response amplitudes at SN were significantly larger in the first half than the second half (paired *t*-test; $t(7)=2.54$, $P=0.039$). The response latency did not differ between the two halves ($t(7)=-0.30$, $P>0.05$).

Figure 6 Time-compressed activity recall. Scatterplot of the physical latency during the conditioning phase (*x* axis) against the recall latency (*y* axis). Filled symbols show data at Post from 5 electrode contacts in which significant reactivations were observed. Error bar indicates 1 SEM across trials within each contact. Data were fitted by a linear regression with a slope of 1/1.54. Dashed line has a slope of 1.0 and originates from (0, 0).

DISCUSSION

Using intracranial electrophysiological recordings, we observed activity recall in awake human early visual cortex after repeated motion stimulation. This effect was consistent with the sequential reactivation observed in visual neural ensembles in rat V1 (Xu et al., 2012).

First, the reactivation was time-compressed compared to the activity evoked by physical stimulation. For spontaneous memory reactivation, the replay was often compressed in time in the hippocampus and neocortex (Foster and Wilson, 2006; Ji and Wilson, 2007). While it has been suggested that the speed of the recalled spike sequence is determined primarily by the network dynamics, the rate of compression may vary in cue-triggered reactivation. In a wakeful state, the compression rate in V1 was found to be ~3 in rat electrophysiological study (Xu et al., 2012), and ~2.3 in human functional magnetic resonance imaging (MRI) study (Ekman et al., 2017). In macaque V4, a sequential image presentation was found to induce a replay with little time compression (Eagleman and Dragoi, 2012). In the present study, the reactivation wave propagated faster than the activity evoked by physical motion. The estimated compression rate was ~1.5. Our results indicate a time-compressed cue-triggered replay in human sensory cortex, consistent with the view that the sequence rather than the time course of the experience is reactivated.

Second, the reactivation was induced by passive conditioning and was triggered by a brief cue without any task. During all the conditioning and test phases, subjects received visual stimulation with no task other than maintaining their central fixation. Such a state resembled the quiet, wakeful, synchronized brain state in rats (Xu et al., 2012) and the unattended awake state in humans (Ekman et al., 2017) in which sequential reactivation has been observed. The sequential reactivation of motion has been also found in anesthetic rats (Xu et al., 2012). These results support the view that sequence learning may be mediated by an automatic synaptic mechanism without top-down voluntary processes.

Third, the conditioning effect decayed rapidly over time. After conditioning, we found that the response amplitude decreased rapidly in ~1.5 min. In Xu et al. (2012), the decay half-life was ~2 min in awake rat V1 following the same number of motion conditioning. Taken together, the above findings suggest that the sequential reactivation in human visual cortex shared many characteristics with previous reported cue-evoked reactivation.

One difference we noted was that the cue-triggered reactivation in space was range-limited. We found a significant reactivation when the cue was presented 4°, but not 8° away from the RF, whereas the activity recall in rat V1 travelled for a longer distance (Xu et al., 2012). A human study has

investigated the same topic—using fMRI and population receptive field mapping, a long-range replay was triggered by a flash at the starting point after familiarizing subjects with a spatial sequence (Ekman et al., 2017). However, their study differed from the present study in both protocol and measurement. During the test phase, the test cues were presented interleavingly with the conditioning sequence. Such protocol would strengthen the conditioning effect, resulting in more resemblance to the long-range conditioning stimuli. Also, fMRI and sEEG measurements reflect different aspects of neural activity. It has been reported that the hemodynamically originated BOLD signal propagates for a longer distance across the cortex (Aquino et al., 2012; Wu et al., 2020), compared to the locally restricted gamma-band activity in the present study (Gabriel and Eckhorn, 2003; Ray and Maunsell, 2011; Sato et al., 2012). Thus, the discrepancy in the range of spatial serial replay might reflect differences in the intrinsic cortical dynamics across species, neural measurement techniques, as well as the stimuli and task-dependent states. This remains to be a topic of interest for future research.

Sequential replay in the sensory cortex constitutes an important form of local neural plasticity. It has been found that a greater amount of V1 reactivation was associated with a greater amount of learning for the trained visual feature (Bang et al., 2018). The cue-triggered motion completion observed in the current study indicates that the early visual cortex contributes to spatiotemporal learning (Gavornik and Bear, 2014; Liu et al., 2019). Our work reflects a growing consensus that high-level learning functions can be implemented in the low-level sensory system (Tsodyks and Gilbert, 2004; Sasaki et al., 2010).

In sum, our data provide electrophysiological evidence for cue-triggered sequential reactivation in early visual cortex in awake human. The current findings reveal a form of short-term neural plasticity and shed light on studying high-level cognition, including prediction, learning, and memory by studying the low-level sensory system.

MATERIALS AND METHODS

Participants

Three subjects (2 females; (35±7.25) years old) who were undergoing clinical intracerebral evaluation for epilepsy participated in the experiment. The small number of subjects in intracranial recordings from occipital cortex is due to the limited accessibility and clinical setting in human intracranial recording. All the participants were right-handed and had normal or corrected-to-normal vision. The participants gave their written consent in accordance with the procedures and protocols approved by the Ethics Committee of the Sanbo Brain Hospital, Capital Medical University.

Receptive field mapping

Prior to the experiment, subjects underwent a receptive field mapping session (Yoshor et al., 2007). Given that all the electrodes were placed in the left hemisphere, RF mapping was performed in the right visual field contralateral to the recording sites. The mapping stimulus was a 3°×3° checkerboard flashed for 500 ms at 1 Hz, reversing in contrast once at 250 ms after each onset. Subjects were asked to fixate at the central point and to detect its color change. In each run, the stimulus was presented at 54 (6×9 grids) positions in the right visual field. VEPs were constructed by averaging all trials for the same location from 5 runs. Contacts were identified as "responsive" if at least one of the recorded VEPs contained significant segments for more than 10 ms during 40–200 ms post stimulus onset (*t*-test against baseline, $P<0.05$, FDR corrected). Eight contacts passed this criterion and were included in further analysis. For responsive electrode contacts, the response at each mapping grid was defined as a root mean square (RMS) deviation from the baseline voltage. We fitted the response map with a two-dimensional Gaussian function. The RF center was defined as the location of the Gaussian peak. The boundary of RF was determined by calculating the root-squared-mean of the full widths at half maximum (FWHM) of the two axes in the fitted Gaussian function. The magnitude of the maximum response was defined by the height of the fitted Gaussian peak.

Stimuli

The conditioning stimulus was a bright dot (3° in diameter, 180 cd m^{-2}) moving at 60°/s from a starting point (S) to an end point (E), along the axis connecting the receptive field and the central fixation point. The visual distance between S and E was 24°, and the estimated RF was the midpoint between S and E. The movement had a duration of 400 ms and was repeated once every 1.8s for 100 times. Before and after conditioning, the same dot briefly flashed for 100 ms at one of four possible points: S, A, B, and E. A and B were the points that divide the line segment between S and RF into three equal parts (Figure 1A). As noted above, the absolute positions of point S/E/A/B were determined according to the RF location, so that the stimuli varied across individual electrode contacts, but the center-to-center distances between the points and RF were constant: S-RF:12°, A-RF: 8°, B-RF: 4°, RF-E: 12°. All visual stimuli were presented on a liquid crystal display (LCD) monitor (53 cm×30 cm, 1920×1080 pixels, 60 Hz) at the bedside in a quiet and dimmed room. Subjects' head was stabilized with a chin rest at a viewing distance of 60 cm.

Procedures

Subjects underwent three phases: (i) pre-test (Pre), (ii) conditioning, (iii) post-test (Post). In the conditioning phase, subjects fixated at the central cross and viewed a white dot moving repeatedly from S to E as described in the Stimuli section. In the test phases, a dot flashed briefly for 100 ms every 1.8 s at the position of either S or B in one block, and at either A or E in the other block. Each block consisted of 100 trials, 50 trials for each condition. All the conditions were presented in a pseudorandom order. At Post, another conditioning was conducted between the two test blocks to prevent the possible decay of the conditioning effect over time. The above procedure was carried out for each recording contact with a specified set of visual stimuli in each subject. Throughout the experiment, subjects were asked to maintain central fixation with no other tasks.

sEEG recordings

Each intracerebral electrode (0.8 mm in diameter) contained 12–18 independent recording contacts of 2 mm in length and 1.5 mm apart from each other. The reference electrode was attached to the skin of each subject's forehead. The cortical reconstruction and segmentation were computed individually based on the T1-weighted image obtained before the electrode implantation using BrainSuite (http://brainsuite.org/). The location of each contact was identified using a post-implantation CT scan co-registered with the pre-implantation T1 image. A visual cortex template (Benson et al., 2014) was applied to the cortical surface reconstructed from the T1 image using FreeSurfer (http://surfer.nmr.mgh.harvard.edu). The intracranial neural responses were collected with the Nicolet clinical amplifier. The sampling rate was 512 Hz in two subjects (S1 and S2) and 2048 Hz in one subject (S3).

sEEG data processing

Preprocessing

Raw sEEG data from each contact were imported into MATLAB (R2019a, MathWorks) and visually inspected for the presence of line noise, recording artifacts, and interictal epileptic spikes. Any epileptic or artifactual channel was excluded from further analysis. Trials that contained voltage values outside the range mean±3 SDs were discarded. Data for S3 were down-sampled to 512 Hz for consistency across subjects.

VEP and spectrogram

VEPs were computed by averaging signals across all trials in the conditioning phase. Then, we conducted a time-frequency analysis of VEPs by convolving signals from responsive electrodes with a series of Morlet wavelets with central frequencies ranging linearly from 10 to 100 Hz. The result of the wavelet transform was used to generate a spectrogram. The time-frequency map was generated with the 1/f compensation (i.e., spectral flattening) using Brainstorm (Tadel et al., 2011). It multiplies the power at each frequency with the frequency value (e.g., the power at 50 Hz was multiplied by 50) to compensate the 1/f decrease in power observed in EEG power spectrum. For pre- and post-conditioning phases, we firstly analyzed the gamma band signal because of its important role in sensory and cognitive processing (Jensen et al., 2007; Bartoli et al., 2019). The raw signals were bandpass filtered at 30–60 Hz (4th order Butterworth, zero-phase filtering). The gamma amplitude was obtained by taking the absolute value of the Hilbert transform. We also analyzed the broadband response by filtering the signals with a bandpass frequency of 8–240 Hz and taking the absolute value of the Hilbert transform. We normalized the amplitude by calculating the percent amplitude change from a −100 to 0 ms pre-stimulus baseline window. Activity latency was quantified as the time from stimulus onset to the maximum amplitude during the 0–200 ms post stimulus onset in individual trials.

Cross-correlogram

A correlation analysis was performed between the time-series responses of each test condition and S (i.e., S-S, S-A, S-B, S-E) across different time lags. Adapted from the method in animal studies (Karlsson and Frank, 2009; Xu et al., 2012), we calculated Pearson correlation coefficients between the averaged gamma-band responses from a sliding window of 195 ms in steps of 15.6 ms for each test condition and the responses from a fixed window (0–195 ms post stimulus onset) for condition S. The correlation coefficients (r) were calculated for each electrode contact and testing phase. Statistical significance of the difference between correlation coefficients was assessed with a permutation test. For each electrode contact and each test condition, we randomly labeled the timeseries responses as Pre or Post for 1,000 times. We recalculated the correlation coefficient difference between Pre and Post (r_{diff}) and yielded a distribution of r_{diff} for each time bin, from which the corresponding threshold values (P=0.05, uncorrected) were obtained. We applied multiple-comparison correction to the uncorrected randomization threshold profile by setting the maximum across all bins as the threshold (Maris and Oostenveld, 2007). Finally, we generated cross-correlograms showing the averaged r^2 across contacts.

Compliance and ethics *The author(s) declare that they have no conflict of interest.*

Acknowledgements *This work was supported by the National Natural*

Science Foundation of China (31971031, 31930053, 31671168, 31421003) and Beijing Municipal Science and Technology Commission (Z181100001518002).

References

Aquino, K.M., Schira, M.M., Robinson, P.A., Drysdale, P.M., and Breakspear, M. (2012). Hemodynamic traveling waves in human visual cortex. PLoS Comput Biol 8, e1002435.

Bahramisharif, A., Jensen, O., Jacobs, J., and Lisman, J. (2018). Serial representation of items during working memory maintenance at letter-selective cortical sites. PLoS Biol 16, e2003805.

Bang, J.W., Sasaki, Y., Watanabe, T., and Rahnev, D. (2018). Feature-specific awake reactivation in human V1 after visual training. J Neurosci 38, 9648–9657.

Bartoli, E., Bosking, W., Chen, Y., Li, Y., Sheth, S.A., Beauchamp, M.S., Yoshor, D., and Foster, B.L. (2019). Functionally distinct gamma range activity revealed by stimulus tuning in human visual cortex. Curr Biol 29, 3345–3358.e7.

Benson, N.C., Butt, O.H., Brainard, D.H., and Aguirre, G.K. (2014). Correction of distortion in flattened representations of the cortical surface allows prediction of V1-V3 functional organization from anatomy. PLoS Comput Biol 10, e1003538.

Bringuier, V., Chavane, F., Glaeser, L., and Frégnac, Y. (1999). Horizontal propagation of visual activity in the synaptic integration field of area 17 neurons. Science 283, 695–699.

Chelaru, M.I., Hansen, B.J., Tandon, N., Conner, C.R., Szukalski, S., Slater, J.D., Kalamangalam, G.P., and Dragoi, V. (2016). Reactivation of visual-evoked activity in human cortical networks. J Neurophysiol 115, 3090–3100.

de Lange, F.P., Heilbron, M., and Kok, P. (2018). How do expectations shape perception? Trends Cogn Sci 22, 764–779.

Deuker, L., Olligs, J., Fell, J., Kranz, T.A., Mormann, F., Montag, C., Reuter, M., Elger, C.E., and Axmacher, N. (2013). Memory consolidation by replay of stimulus-specific neural activity. J Neurosci 33, 19373–19383.

Eagleman, S.L., and Dragoi, V. (2012). Image sequence reactivation in awake V4 networks. Proc Natl Acad Sci USA 109, 19450–19455.

Ekman, M., Kok, P., and de Lange, F.P. (2017). Time-compressed preplay of anticipated events in human primary visual cortex. Nat Commun 8, 1–9.

Fortin, N.J., Agster, K.L., and Eichenbaum, H.B. (2002). Critical role of the hippocampus in memory for sequences of events. Nat Neurosci 5, 458–462.

Foster, D.J. (2017). Replay comes of age. Annu Rev Neurosci 40, 581–602.

Foster, D.J., and Wilson, M.A. (2006). Reverse replay of behavioural sequences in hippocampal place cells during the awake state. Nature 440, 680–683.

Gabriel, A., and Eckhorn, R. (2003). A multi-channel correlation method detects traveling γ-waves in monkey visual cortex. J Neurosci Methods 131, 171–184.

Gavornik, J.P., and Bear, M.F. (2014). Learned spatiotemporal sequence recognition and prediction in primary visual cortex. Nat Neurosci 17, 732–737.

Gelbard-Sagiv, H., Mukamel, R., Harel, M., Malach, R., and Fried, I. (2008). Internally generated reactivation of single neurons in human hippocampus during free recall. Science 322, 96–101.

Han, F., Caporale, N., and Dan, Y. (2008). Reverberation of recent visual experience in spontaneous cortical waves. Neuron 60, 321–327.

Huang, Q., Jia, J., Han, Q., and Luo, H. (2018). Fast-backward replay of sequentially memorized items in humans. eLife 7, e35164.

Jafarpour, A., Fuentemilla, L., Horner, A.J., Penny, W., and Duzel, E. (2014). Replay of very early encoding representations during recollection. J Neurosci 34, 242–248.

Jensen, O., Kaiser, J., and Lachaux, J.P. (2007). Human gamma-frequency oscillations associated with attention and memory. Trends Neurosci 30, 317–324.

Ji, D., and Wilson, M.A. (2007). Coordinated memory replay in the visual cortex and hippocampus during sleep. Nat Neurosci 10, 100–107.

Karlsson, M.P., and Frank, L.M. (2009). Awake replay of remote experiences in the hippocampus. Nat Neurosci 12, 913–918.

Lisman, J.E., and Jensen, O. (2013). The theta-gamma neural code. Neuron 77, 1002–1016.

Liu, Y., Dolan, R.J., Kurth-Nelson, Z., and Behrens, T.E.J. (2019). Human replay spontaneously reorganizes experience. Cell 178, 640–652.e14.

Maris, E., and Oostenveld, R. (2007). Nonparametric statistical testing of EEG- and MEG-data. J Neurosci Methods 164, 177–190.

Ray, S., and Maunsell, J.H.R. (2011). Different origins of gamma rhythm and high-gamma activity in macaque visual cortex. PLoS Biol 9, e1000610.

Sasaki, Y., Nanez, J.E., and Watanabe, T. (2010). Advances in visual perceptual learning and plasticity. Nat Rev Neurosci 11, 53–60.

Sato, W., Kochiyama, T., Uono, S., Matsuda, K., Usui, K., Inoue, Y., and Toichi, M. (2012). Temporal profile of amygdala gamma oscillations in response to faces. J Cogn Neurosci 24, 1420–1433.

Tadel, F., Baillet, S., Mosher, J.C., Pantazis, D., and Leahy, R.M. (2011). Brainstorm: a user-friendly application for MEG/EEG analysis. Comput Intell Neurosci 2011, 1–13.

Tallon-Baudry, C., and Bertrand, O. (1999). Oscillatory gamma activity in humans and its role in object representation. Trends Cogn Sci 3, 151–162.

Tsodyks, M., and Gilbert, C. (2004). Neural networks and perceptual learning. Nature 431, 775–781.

Wilson, M.A., and McNaughton, B.L. (1994). Reactivation of hippocampal ensemble memories during sleep. Science 265, 676–679.

Wu, D., Li, X., and Jiang, T. (2020). Reconstruction of behavior-relevant individual brain activity: an individualized fMRI study. Sci China Life Sci 63, 410–418.

Xu, S., Jiang, W., Poo, M.M., and Dan, Y. (2012). Activity recall in a visual cortical ensemble. Nat Neurosci 15, 449–455.

Yao, H., Shi, L., Han, F., Gao, H., and Dan, Y. (2007). Rapid learning in cortical coding of visual scenes. Nat Neurosci 10, 772–778.

Yoshor, D., Bosking, W.H., Ghose, G.M., and Maunsell, J.H.R. (2007). Receptive fields in human visual cortex mapped with surface electrodes. Cereb Cortex 17, 2293–2302.

Zhang, Y., Zhang, Y.Y., and Fang, F. (2020). Neural mechanisms of feature binding. Sci China Life Sci 63, 926–928.

SUPPORTING INFORMATION

The supporting information is available online at https://doi.org/10.1007/s11427-020-1726-5. The supporting materials are published as submitted, without typesetting or editing. The responsibility for scientific accuracy and content remains entirely with the authors.